J Appl Physiol 104: 423–428, 2008.
First published December 13, 2007; doi:10.1152/japplphysiol.00884.2007.

Mechanics of the canine diaphragm in ascites: a CT study

Dimitri Leduc,[1,2] Matteo Cappello,[1,2] Pierre Alain Gevenois,[3] and André De Troyer[1,2]

[1]*Laboratory of Cardiorespiratory Physiology, Brussels School of Medicine,* [2]*Chest Service, and* [3]*Department of Radiology, Erasme University Hospital, Brussels, Belgium*

Submitted 17 August 2007; accepted in final form 13 November 2007

Leduc D, Cappello M, Gevenois PA, De Troyer A. Mechanics of the canine diaphragm in ascites: a CT study. *J Appl Physiol* 104: 423–428, 2008. First published December 13, 2007; doi:10.1152/japplphysiol.00884.2007.—Ascites causes an increase in the elastance of the abdomen and impairs the lung-expanding action of the diaphragm, but its overall effects on the pressure-generating ability of the muscle remain unclear. In the present study, radiopaque markers were attached to muscle bundles in the midcostal region of the diaphragm in five dogs, and the three-dimensional locations of the markers during relaxation and during phrenic nerve stimulation in the presence of increasing amounts of ascites were determined using a computed tomographic scanner. From these data, accurate measurements of muscle length and quantitative estimates of diaphragm curvature were obtained, and the changes in transdiaphragmatic pressure (Pdi) were analyzed as functions of muscle length and curvature. With increasing ascites, the resting length of the diaphragm increased progressively. In addition, the amount of muscle shortening during phrenic nerve stimulation decreased gradually. When ascites was 100 ml/kg body wt, therefore, the muscle during contraction was longer, leading to a 20–25% increase in Pdi. As ascites increased further to 200 ml/kg, however, muscle length during contraction continued to increase, but Pdi did not. This absence of additional increase in Pdi was well explained by the increase in the diameter of the ring of insertion of the diaphragm to the rib cage and the concomitant increase in the radius of diaphragm curvature. These observations indicate that the pressure-generating ability of the diaphragm is determined not only by muscle length as conventionally thought but also by muscle shape.

respiratory muscles; length-tension characteristics; diaphragm curvature; mechanics of breathing; computed tomography

ASCITES, A COMPLICATING FEATURE of many diseases of the liver and peritoneum, commonly causes dyspnea (1, 3, 16). In an attempt to evaluate the role played by the respiratory muscles in the occurrence of this symptom, we recently developed a model of ascites in dogs and measured the fall in airway opening pressure (ΔPao) during selective stimulation of the phrenic nerves in the presence of increasing amounts of liquid in the abdominal cavity (12). Results indicated that ascites, as a primary effect, causes an increase in the elastance of the abdominal compartment of the respiratory system and impairs the lung-expanding action of the diaphragm. In a second set of experiments, we showed that this impairment, in turn, elicits a compensatory increase in neural drive to the inspiratory muscles, in particular the parasternal intercostals. However, the compensation was not sufficient, so that tidal volume was reduced and arterial P_{CO_2} was increased. Based on the conventional current theory of dyspnea (2, 13), it was therefore concluded that the symptom in ascites results in part from the dissociation between increased neural drive and decreased ventilation (12).

The precise impact of ascites on diaphragm function, however, remained unclear. Thus radiographic measurements of diaphragm silhouette showed, in agreement with the increase in abdominal elastance, that the caudal displacement of the muscle during phrenic nerve stimulation decreased gradually as the amount of liquid in the abdominal cavity increased (12). Apparently, therefore, the loss in ΔPao could be explained. However, with such a decrease in diaphragm displacement, it would be expected that the active muscle fibers would be longer and, consequently, that the muscle would develop greater force in response to a given activation. Instead, when ascites was severe, the rise in transdiaphragmatic pressure (ΔPdi) during phrenic stimulation was also reduced, thus suggesting that a mechanism other than the increase in abdominal elastance was operating. The hypothesis was considered that this mechanism was related to the expansion of the lower rib cage, but the measured decrease in ΔPdi appeared disproportionately greater (12).

The objective of the present study was to determine the effect of ascites on the overall pressure-generating ability of the diaphragm and to assess the mechanism(s) of this effect. Radiopaque markers were attached along muscle bundles in the midcostal region of the diaphragm in dogs, and the animals were placed in a computed tomographic (CT) scanner. Consequently, accurate measurements of muscle length during ascites were obtained, and quantitative estimates of diaphragm curvature were computed. The roles of the muscle length-tension properties and muscle shape in determining the pressure changes with ascites, therefore, could be clarified.

METHODS

The studies were carried out on five adult cross-breed dogs (19–24 kg) anesthetized with pentobarbital sodium (initial dose, 30 mg/kg iv), as approved by the Animal Ethics and Welfare Committee of the Brussels School of Medicine. The animals were placed in the supine position, intubated with a cuffed endotracheal tube, and connected to a mechanical ventilator (Harvard Pump, Chicago, IL). A venous cannula was inserted in the forelimb to give maintenance doses of anesthetic, after which the abdomen was opened by a midline incision from the xiphisternum to the umbilicus and rows of polyethylene spheres (3–4 mm in diameter with a small hole drilled through the center) were stitched superficially to a muscle bundle in the midcostal region of both the left and the right hemidiaphragm. Five to six markers were placed 15–30 mm apart along each muscle bundle: one at the origin of the bundle on the central tendon, one at its insertion into the ribs, and three to four at equal intervals between these two. Consequently, the chord length between the successive markers

Address for reprint requests and other correspondence: A. De Troyer, Chest Service, Erasme Univ. Hospital, 808, route de Lennik, 1070 Brussels, Belgium (e-mail: a_detroyer@yahoo.fr).

The costs of publication of this article were defrayed in part by the payment of page charges. The article must therefore be hereby marked "*advertisement*" in accordance with 18 U.S.C. Section 1734 solely to indicate this fact.

closely approximated the arc length along the diaphragm. In each animal, a balloon-catheter system filled with 1.0 ml of air was also placed between the liver and the stomach to measure abdominal pressure (Pab), and a polyethylene tubing was inserted through the right external oblique and internal oblique muscles of the abdomen, midway between the costal margin and the iliac crest, such that liquid could easily be introduced into the abdominal cavity later. After the abdomen was closely sutured in two layers, the C_5 and C_6 phrenic nerve roots were isolated bilaterally in the neck.

After a 30-min recovery period, the animal was transferred to a V-shaped board and placed in a four-channel multidetector CT scanner (Somatom Volume Zoom 4, Siemens Medical Solutions, Forchheim, Germany). Foam pillows were placed in the board on both sides of the cranial portion of the rib cage to stabilize further the animal position within the scanner, after which the C_5 and C_6 phrenic nerve roots were laid over two pairs of insulated stainless steel stimulating electrodes. A differential pressure transducer (Validyne, Northridge, CA) was also connected to a side port of the endotracheal tube to measure the changes in airway opening pressure (ΔPao). The rate of the ventilator was then increased to 30–35 strokes/min for 5–10 min to make the animal apneic, and a first helical data acquisition starting ~3 cm caudal to the lower rib cage margin and extending to ~2 cm cranial to the xiphoid process was performed during relaxation at functional residual capacity (FRC). Preliminary experiments showed that the following scanning parameters allowed precise display of the diaphragm markers: 120 kV, 120 effective mA, 0.5 s/revolution scanning time, 1-mm collimation, and 6.9 mm feed/rotation. Depending on the size of the animal, therefore, the distance covered with one scan ranged from 94 to 123 mm and the acquisition lasted 7–9 s.

After the first acquisition was completed, the animal was reconnected to the ventilator and hyperventilated again. After the ventilator was stopped, the endotracheal tube was occluded at FRC, and square pulses of 0.1-ms duration and supramaximal voltage were applied at a frequency of 20 impulses/s to the left and right phrenic nerves. A second CT data acquisition was obtained at this time, and the ΔPao and ΔPab generated by the stimulation were recorded. A volume of 50 ml isosmotic liquid (Dianeal glucose 1.36%, Baxter) per kilogram body weight was then introduced into the abdominal cavity, and after a 10- to 15-min recovery period, a new set of data was obtained, first during relaxation and then during phrenic nerve stimulation. The value of Pab during relaxation in the presence of ascites was also measured; it was expressed relative to the value before ascites (control). Liquid volume was subsequently increased by increments of 50 ml/kg body wt up to a total of 200 ml/kg, and the measurements were repeated at each volume.

The animals were maintained at a constant, rather deep level of anesthesia throughout the study with supplemental doses of pentobarbital sodium (2–3 $mg \cdot kg^{-1} \cdot h^{-1}$). Thus, at no time in the experiment, including during phrenic nerve stimulation, did they have a corneal reflex or movements of the fore- or hindlimbs,. Rectal temperature was maintained constant between 36 and 38°C with infrared lamps. At the conclusion of the experiment, the animal was given an overdose of anesthetic (30–40 mg/kg iv).

Data analysis. For each volume of ascites, 1.25 mm thick transverse CT sections during relaxation and during phrenic nerve stimulation were reconstructed at 1.0-mm intervals by using a 360° linear-interpolation algorithm and a standard kernel (AB 40 f, Siemens Medical Solutions); a total of 100–110 successive transverse images were therefore obtained for each acquisition. Sagittal and coronal images were also reconstructed, and these multiplanar reformations of the diaphragm were then used in a workstation (Leonardo, Siemens Medical Solutions) to measure diaphragm length. Thus, for each muscle bundle (i.e., each hemidiaphragm) in each condition, the point corresponding to the cranial edge of the marker situated near the central tendon was carefully defined, and the three-dimensional coordinates of the point were recorded. By using the transverse, coronal and sagittal images, the cranial edge of the adjacent marker was next defined, and the three-dimensional coordinates of this point were also recorded such that the linear distance between the two markers could be computed and expressed in millimeters. The linear distances between the other markers in the row were measured similarly, and the length of the hemidiaphragm was obtained by summing the four or five distances between the five or six markers. To allow comparison between the different animals, muscle lengths during relaxation with ascites and during phrenic nerve stimulation were then expressed as percentages of muscle length during relaxation in the control condition (L_{FRC}).

Two additional measurements were performed on the basis of the CT images. *1*) The curvature of the diaphragm during phrenic nerve stimulation was quantified by using the multiplanar reformations of the muscle. That is, for each hemidiaphragm in each condition, a plane was fit to the five or six markers in the row, and chords tangent to the markers were constructed in the plane between the top three pairs of markers. Normals to the chords were then constructed at midchord points, and the radius of diaphragm curvature was measured from the intersection of the normals. It is worth pointing out that no reliable estimate of the radius of curvature during relaxation could be made with this procedure. Indeed, whereas during phrenic nerve stimulation, three to four markers in the row were consistently away from the rib cage, during relaxation, all but one or two markers were apposed to the rib cage (14). *2*) The inner transverse diameter of the rib cage during phrenic nerve stimulation was measured by using the transverse CT scan obtained at the level of the two markers situated near the muscle insertions into the ribs.

Statistical analysis. There were no consistent differences in length or curvature between the right and left hemidiaphragms. Also, there were no consistent interhemidiaphragmatic differences in the positions of the markers situated near the central tendon or at the muscle insertions into the ribs. For each condition, therefore, the values for the two hemidiaphragms were averaged for each individual animal, and they were then averaged across the animal group. The values of ΔPao, Pab, and transverse rib cage diameter were also averaged across the animal group, and they are presented as means ± SE. Statistical assessments of the effects of increasing ascites on pressure, marker positions, muscle length, radius of curvature, and transverse rib cage diameter were made by ANOVA with repeated measures, and multiple comparison testing of the mean values was performed, when appropriate, using Student-Newman-Keuls tests. The criterion for statistical significance was taken as $P < 0.05$.

RESULTS

Pressure. The effects of increasing ascites on the value of Pab during relaxation are shown for the five animals in Fig. 1*A*, and the values of ΔPao and ΔPab obtained during phrenic nerve stimulation are shown in Fig. 1*B*. With increasing ascites, the resting Pab increased gradually in every animal ($P < 0.001$). The rise in Pab during phrenic nerve stimulation also increased progressively ($P < 0.001$) as ascites increased to 150 ml/kg, and it then remained unchanged as ascites increased further. In contrast, ΔPao decreased markedly as ascites increased from 100 to 200 ml/kg ($P < 0.001$). As a result, ΔPdi increased, although not significantly, from 52.5 ± 4.7 cmH_2O in the control condition to 60.8 ± 3.4 cmH_2O in the presence of 100 ml/kg ascites, and it then decreased to 45.9 ± 3.2 cmH_2O as ascites increased to 200 ml/kg ($P < 0.05$).

Position and length of the diaphragm. The anterior-posterior view of the diaphragm markers during relaxation and during phrenic nerve stimulation in the control condition and in the presence of 200 ml/kg ascites is shown for a representative animal in Fig. 2, and the axial position of the markers situated near the central tendon and at the muscle insertions into the ribs

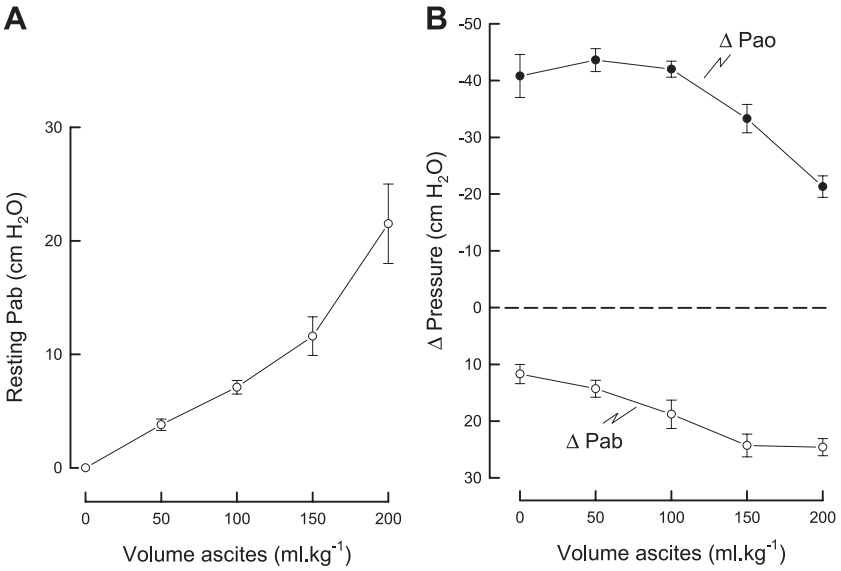

Fig. 1. Abdominal pressure (Pab) during relaxation (*A*) and changes in airway opening pressure (ΔPao) and Pab (ΔPab) during bilateral stimulation of the C_5 and C_6 phrenic nerve roots (*B*) in the presence of different volumes of ascites. Values are means ± SE obtained from 5 animals. Pab during relaxation was adjusted to yield a value of 0 cmH_2O in the control condition. The vertical distance between ΔPao and ΔPab at a given volume of ascites in *B* corresponds to the change in transdiaphragmatic pressure (ΔPdi); note that ΔPdi increased as ascites increased from 0 to 100 ml/kg but then decreased as ascites increased further.

in the five animals in all conditions is shown in Fig. 3. With the animal relaxed, the markers situated near the central tendon were gradually displaced in the cranial direction as ascites increased ($P < 0.001$). The muscle insertions into the ribs were also displaced cranially, and this displacement was similar in magnitude to that of the central tendon. With ascites, however, the muscle insertions into the ribs were also displaced outward (Fig. 2). As a result, the muscle fibers lengthened progressively ($P < 0.001$), and when ascites amounted to 200 ml/kg, they were 13.3 ± 1.3% longer than in the control condition (Fig. 4).

Phrenic nerve stimulation in all conditions caused a large shortening of the muscle fibers and a large caudal displacement of the central tendon as well as a caudal displacement of the muscle insertions into the ribs. As shown in Fig. 3, however, the caudal displacement of the tendon and the muscle insertions into the ribs decreased as ascites increased ($P < 0.001$ for both). The amount of muscle shortening also decreased ($P < 0.001$), and muscle length during contraction increased ($P < 0.001$) (Fig. 4). Thus, whereas active muscle length in the control condition was 60.8 ± 1.1% of L_{FRC}, with 200 ml/kg ascites, it was 81.3 ± 2.7%.

Diaphragm curvature. Figure 5*A* shows the values of the radius of diaphragm curvature during phrenic nerve stimulation in the different conditions. The radius of curvature in every animal was 3–5 cm during control, in agreement with the earlier estimates of Kim et al. (11) and the recent measurements of Boriek et al. (4, 5), and it remained unchanged in the presence of 50 ml/kg ascites. As ascites increased from 50 to 150 ml/kg, however, although the variation between the dif-

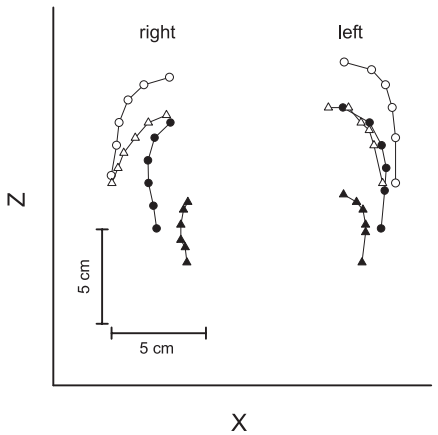

Fig. 2. Anterior-posterior view of marker locations in the right and left hemidiaphragms obtained for a representative animal during relaxation in the control condition (●) and in the presence of 200 ml/kg ascites (○) and during phrenic nerve stimulation in the same conditions (▲ and △, respectively). The *x*-axis lies in the laterolateral direction, and the *z*-axis lies in the craniocaudal direction. Note the cranial displacement of the relaxed diaphragm with ascites as well as the cranial and outward displacement of the costal insertions of the muscle. During stimulation, the muscle fibers shortened and the diaphragm moved caudally, more markedly so in the control condition than in the presence of ascites.

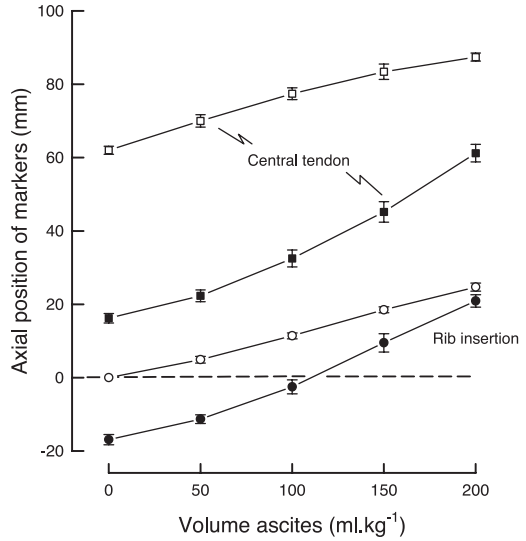

Fig. 3. Axial position of the diaphragm markers situated near the central tendon (squares) and the muscle insertions into the ribs (circles) during relaxation (open symbols) and during phrenic nerve stimulation (filled symbols) in the presence of different volumes of ascites. Values are means ± SE obtained from 5 animals. The marker positions are expressed relative to the position of the rib markers during relaxation in the control condition; positive values indicate cranial position and negative values indicate caudal position.

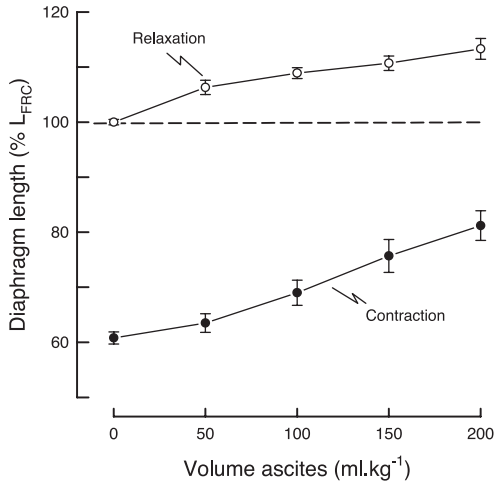

Fig. 4. Diaphragm muscle length during relaxation (○) and during phrenic nerve stimulation (●) in the presence of different volumes of ascites. Values are means ± SE obtained from 5 animals, All values are expressed as percentages of muscle length during relaxation in the control condition (L_{FRC}). Note the increase in relaxed and active muscle length with increasing ascites.

ferent animals was larger, the radius of curvature increased gradually ($P < 0.001$). At 200 ml/kg, therefore, it amounted to 6.0 ± 0.6 cm.

The transverse diameter of the lower rib cage also increased progressively and consistently with increasing ascites ($P < 0.001$). As shown in Fig. 5*B*, the diameter in the control condition was 13.16 ± 0.47 cm, but it was 16.50 ± 1.00 cm with 100 ml/kg ascites and 18.31 ± 0.55 cm with 200 ml/kg.

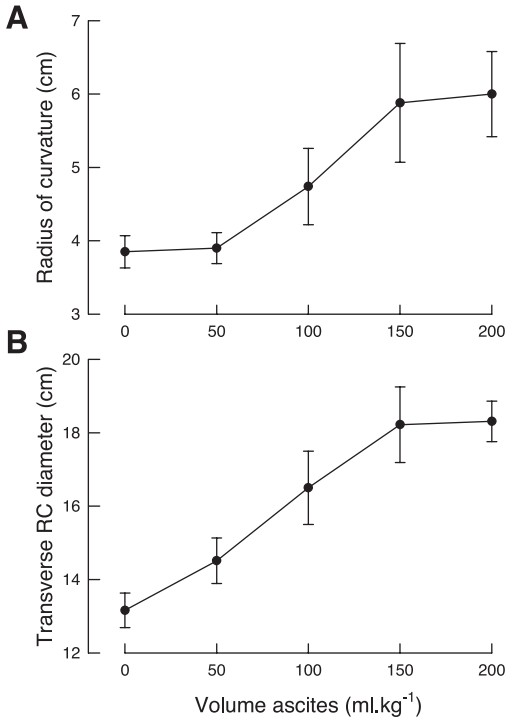

Fig. 5. Values of the radius of diaphragm curvature (*A*) and the transverse diameter of the lower rib cage (RC; *B*) during phrenic nerve stimulation in the presence of different volumes of ascites. Values are means ± SE obtained from 5 animals.

DISCUSSION

The observations made in this study confirmed our previous finding (12) that the ΔPao produced by a given activation of the diaphragm decreases in the presence of severe ascites. These observations also confirmed that despite the marked increase in abdominal elastance, this loss in ΔPao is not compensated for by an increase in ΔPab, such that ΔPdi also decreases (Fig. 1B). However, whereas in our previous study, radiopaque markers were attached in the coronal midplane so as to evaluate diaphragm silhouette with anterior-posterior radiographs (12), in the present study, the markers were attached along muscle bundles in the midcostal portion of the diaphragm and the three-dimensional positions of the markers were assessed by using CT. Thus, in the present study, we could make accurate measurements of muscle length despite the fact that the muscle fibers of the midcostal diaphragm run both laterally and ventrally from their origin on the central tendon to their insertions into the ribs. In addition, we could obtain quantitative estimates of muscle curvature. Consequently, the effects of ascites on the passive and active diaphragm could be determined.

Effects of ascites on the passive diaphragm. It is well established that in supine dogs, the relaxed diaphragm at FRC is close to the in vitro optimum force-producing length (L_o) of the muscle (9, 15). At L_o, the muscle generates passive tension and offers a significant resistance to lengthening (11, 15). With increasing ascites, however, the relaxed diaphragm in our animals progressively lengthened (Fig. 4) as the resting Pab increased (Fig. 1*A*). The values of diaphragm length measured during relaxation at the different volumes of ascites are plotted against the corresponding values of resting Pab in Fig. 6 (filled circles). In agreement with the passive length-tension charac-

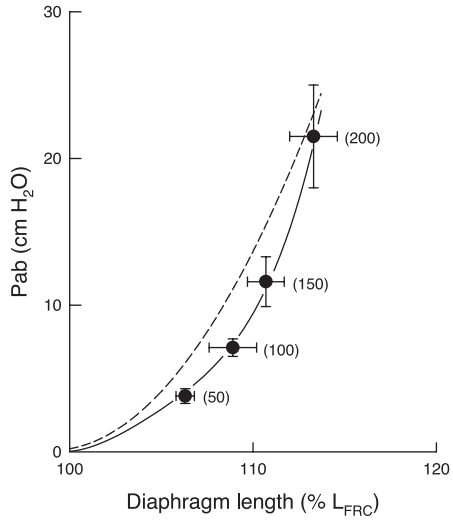

Fig. 6. Relationship between Pab and diaphragm muscle length during relaxation in the presence of different volumes of ascites. ●, Mean ± SE values obtained from the 5 animals of the study; solid line, relationship computed from these data. Diaphragm muscle length is expressed as a percentage of L_{FRC}, and the numbers next to the circles refer to the volume of ascites expressed as ml/kg body wt. Dashed line, aggregate passive length-Pab curve previously obtained for the costal and crural portions of the canine diaphragm by Road et al. (15). [Note that because Pab in our animals was adjusted to yield 0 cmH_2O in the control condition, for the sake of comparison, the curve reported by Road et al. (15) was redrawn by considering that Pab at optimum force-producing length was also zero.]

teristics of skeletal muscles, the relationship between these values (solid line) was curvilinear, such that for a given increase in Pab, the amount of muscle lengthening decreased as Pab was greater. Also, this relationship was well matched with the passive diaphragm length-Pab curve previously obtained during external compression of the abdomen in dogs by Road et al. (15) (dashed line). In contrast to the present study, however, these animals had a rigid cast placed around the lower rib cage, such that the ribs and sternum remained stationary during compression.

Diaphragm lengthening is, as a first approximation, proportional to the relative displacement of the dome and the muscle insertions into the ribs. That is, for a given muscle lengthening, the cranial displacement of the dome of the diaphragm should be larger if the insertions into the ribs move cranially than it would be if the insertions did not move. Hubmayr et al. (10) previously observed that in supine dogs, introducing 60–100 ml/kg Ringer solution into the abdominal cavity induced a substantial cranial displacement of both the dome of the diaphragm and the muscle insertions into the ribs. Similarly, as is shown in Fig. 3, the animals in the present study showed a gradual cranial displacement of the costal insertions of the diaphragm with increasing ascites. In fact, this displacement was similar in magnitude to the cranial displacement of the dome, which leads to the conclusion that the cranial displacement of the dome with ascites is the result of both the increase in length of the muscle fibers and the cranial displacement of the muscle insertions into the ribs.

Effects of ascites on the active diaphragm. In agreement with our previous radiographic evaluation (12), the CT measurements in this study showed that the descent of the diaphragmatic dome during phrenic nerve stimulation decreased with increasing ascites (Fig. 3). These measurements, however, had an unexpected feature: with phrenic nerve stimulation, the muscle insertions into the lower ribs moved caudally in the control condition, and this caudal displacement, albeit smaller, persisted in the presence of ascites. We have previously found that isolated, supramaximal phrenic nerve stimulation in dogs with the airway open displaces the most caudal ribs in the caudal direction (8). Indeed, shortening of the diaphragm during supramaximal phrenic nerve stimulation is such that the zone of apposition all but disappears, and the muscle fibers from their insertions into the ribs run transversally inward as well as cranially (6, 7). As a result, the inspiratory effect of Pab on the lower rib cage is lost, the entire rib cage is exposed to pleural pressure (Ppl), and the so-called "insertional" force of the diaphragm has become expiratory. With severe ascites, however, the descent of the diaphragm is impeded, ΔPab is greater, and the change in Ppl (ΔPpl) is smaller. Therefore, we expected that the diaphragm markers situated near the muscle insertions into the lower ribs would move cranially. Apparently, although the descent of the dome was smaller in the presence of ascites, the zone of apposition was still markedly reduced, and the insertional force of the diaphragm remained insufficient to overcome ΔPpl.

The displacement of the lower ribs during phrenic stimulation should affect the displacement of the dome in much the same way as it does during relaxation. Thus, for a given muscle shortening, the caudal displacement of the dome should be larger if the insertions into the ribs move caudally than it would be if the insertions did not move. In view of the observed decrease in the caudal displacement of the insertions with increasing ascites (Fig. 3), it can therefore be concluded that this decrease made a significant contribution to the decrease in the caudal displacement of the dome and, with it, to the decrease in ΔPao.

Irrespective of the displacement of the diaphragmatic insertions into the ribs, severe ascites caused a reduction in the amount of muscle shortening during phrenic nerve stimulation, and this reduction added to the increase in resting muscle length such that the muscle during contraction was longer (Fig. 4). Specifically, whereas muscle length during stimulation in the control condition was 61% of the resting FRC length, in the presence of 200 ml/kg ascites, it was 81%. Based on this value, one may therefore conclude that in the presence of severe ascites, the active diaphragm, although longer, continued to operate on the ascending portion of its length-tension curve. Moreover, because in supine dogs, passive diaphragm tension appears at a muscle length corresponding to ~80% L_o (11, 15), one may also conclude that with ascites, the effective pressure developed by the muscle (Pdi) during contraction consisted of the sum of the ΔPdi measured during contraction and the resting Pab. Consequently, in this setting, the relationship between Pdi and muscle length can be assessed with precision.

The values of active Pdi calculated for the different conditions of the study are plotted against the corresponding values of active muscle length in Fig. 7, and these data are compared with the active Pdi-length curve obtained by Road et al. (15). The data point corresponding to the control condition in our animals was very close to that curve. With 50 and 100 ml/kg ascites, the animals showed a moderate increase in active muscle length and, in agreement with the previous observation by Hubmayr et al. (10), a 20–25% increase in active Pdi. The data points corresponding to these two volumes of ascites were

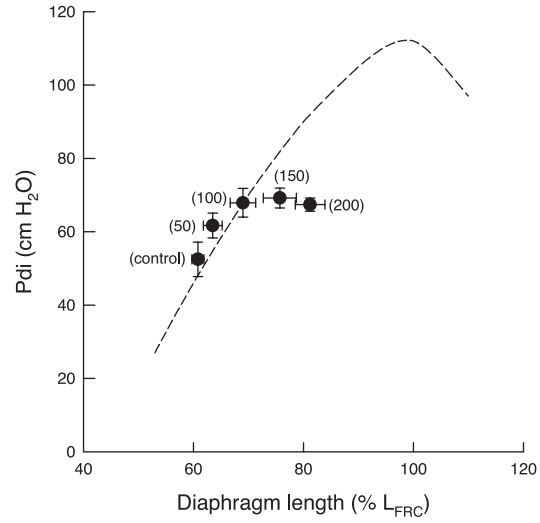

Fig. 7. Relationship between active Pdi and diaphragm muscle length during phrenic nerve stimulation in the presence of different volumes of ascites. ●, Mean ± SE values obtained from the 5 animals of the study; and the numbers next to the circles refer to the volume of ascites expressed as ml/kg body wt. Muscle length is expressed as a percentage of L_{FRC}, and the dashed line is the active length-tension curve reported for the canine diaphragm in vivo by Road et al. (15). Note that the data points obtained in our animals during control and in the presence of 50 and 100 ml/kg ascites are close to the length-tension curve of Road et al. The data points obtained with 150 and 200 ml/kg ascites, however, lay well below the curve.

also close to the curve reported by Road et al. (15). However, as ascites increased to 150 and 200 ml/kg, active muscle length increased further, but active Pdi stopped increasing, such that the data points lie well below the curve. In other words, the increase in active Pdi observed in the presence of moderate amounts of ascites is primarily the result of the increase in active muscle length, but Pdi in the presence of severe ascites is smaller than anticipated on the basis of muscle length.

In recent studies, Boriek et al. (4, 5) measured the changes in diaphragm muscle length and the changes in diaphragm curvature during spontaneous inspiratory efforts and during isolated phrenic nerve stimulation at different lung volumes in dogs. During inspiratory efforts, muscle length decreased to 85–60% of the resting FRC length, and curvature remained unchanged. During phrenic nerve stimulation, however, the radius of diaphragm curvature increased sharply as muscle length decreased further to 55–60%. Based on these observations, these investigators concluded that Pdi during spontaneous inspiratory efforts is exclusively determined by muscle length but that Pdi during phrenic nerve stimulation is determined by both muscle length and curvature. Boriek et al. also explained the change in curvature by a simple geometric model in which the diaphragm is pictured as a circular arc that extends between the attachments on opposite sides of the rib cage (as the muscle shortens, the radius of the arc stays nearly constant for a range of muscle shortening and then increases rapidly as shortening increases further), and they noted that the radius of curvature would increase if the diameter of the rib cage increased.

In agreement with these ideas, our animals had a gradual increase in the radius of diaphragm curvature with increasing ascites (Fig. 5*A*). Moreover, this increase was approximately commensurate with an increase in the transverse diameter of the rib cage (Fig. 5*B*). In addition, and perhaps more important, when ascites was 200 ml/kg, the radius of curvature was 56% greater than that in the control condition. On the basis of Laplace's law, which states that for a given tension Pdi is inversely related to the radius of diaphragm curvature, it would therefore be expected that Pdi with 200 ml/kg ascites would be 1/1.56 or 0.64 times the value that would be obtained for the same muscle length if the radius of curvature remained constant. Thus, if the increase in the radius of curvature played a major role in preventing Pdi from increasing with severe ascites, the pressure loss would be ~35%. The observed loss in Pdi was, in fact, 28% (Fig. 7), and this quantitative matching provides strong support to the idea that the alteration in diaphragm curvature is the primary determinant of the loss in Pdi in this condition. It should be pointed out, however, that the radius of diaphragm curvature in our animals was much less than half the diameter of the lower rib cage (Fig. 5), thus indicating that the relationship between muscle curvature and rib cage diameter is more complex than in the model of Boriek et al. (4).

In summary, the observations reported in this study suggest that ascites affects the pressure-generating ability of the diaphragm by two mechanisms operating simultaneously. First, ascites lengthens the relaxed diaphragm and increases the load on the muscle. As a result, the muscle fibers during contraction are longer and their pressure-generating ability is enhanced, but the lung-expanding action of the muscle is impaired. Second, ascites also expands the ring of insertion of the diaphragm to the lower rib cage and induces a decrease in diaphragm curvature. In the presence of severe ascites, therefore, although the muscle during contraction is even longer, its pressure-generating ability no longer increases.

ACKNOWLEDGMENTS

The authors are grateful to T. A. Wilson (University of Minnesota, Minneapolis, MN) for helpful discussions.

GRANTS

This study was financially supported by Fonds National de la Recherche Scientifique (Belgium) Grants 3.4558.06 F and 3.4566.08.

REFERENCES

1. **Abelmann WH, Frank NR, Gaensler EA, Cugell DW.** Effects of abdominal distension by ascites on lung volumes and ventilation. *Arch Intern Med* 93: 528–540, 1954.
2. **American Thoracic Society.** Dyspnea: mechanisms, assessment, and management. *Am J Respir Crit Care Med* 159: 321–340, 1999.
3. **Bender MD.** Diseases of the peritoneum. In: *Cecil Textbook of Medicine* (18th ed.), edited by Wyngaarden JB and Smith KH Jr. Philadelphia, PA: Saunders, 1988, p. 790–795.
4. **Boriek AM, Black B, Hubmayr R, Wilson TA.** Length and curvature of the dog diaphragm. *J Appl Physiol* 101: 794–798, 2006.
5. **Boriek AM, Rodarte JR, Wilson TA.** Kinematics and mechanics of midcostal diaphragm of dog. *J Appl Physiol* 83: 1068–1075, 1997.
6. **De Troyer A, Cappello M, Meurant N, Scillia P.** Synergism between the canine left and right hemidiaphragms. *J Appl Physiol* 94: 1757–1765, 2003.
7. **De Troyer A, Cappello M, Scillia P.** Effect of inflation on the interaction between the left and right hemidiaphragms. *J Appl Physiol* 99: 1301–1309, 2005.
8. **De Troyer A, Leduc D.** Effect of diaphragmatic contraction on the action of the canine parasternal intercostals. *J Appl Physiol* 101: 169–175, 2006.
9. **Farkas GA, Rochester DF.** Functional characteristics of canine costal and crural diaphragm. *J Appl Physiol* 65: 2253–2260, 1988.
10. **Hubmayr RD, Sprung J, Nelson S.** Determinants of transdiaphragmatic pressure in dogs. *J Appl Physiol* 69: 2050–2056, 1990.
11. **Kim MJ, Druz WS, Danon J, Machnach W, Sharp JT.** Mechanics of the canine diaphragm. *J Appl Physiol* 41: 369–382, 1976.
12. **Leduc D, De Troyer A.** Dysfunction of the canine respiratory muscle pump in ascites. *J Appl Physiol* 102: 650–657, 2007.
13. **Manning HL, Schwartzstein RM.** Pathophysiology of dyspnea. *N Engl J Med* 333: 1547–1553, 1995.
14. **Mead J.** Functional significance of the area of apposition of diaphragm to rib cage. *Am Rev Respir Dis* 119: 31–32, 1979.
15. **Road J, Newman S, Derenne JP, Grassino A.** In vivo length-force relationship of canine diaphragm. *J Appl Physiol* 60: 63–70, 1986.
16. **Sherlock S, Dooley J.** Ascites. In: *Diseases of the Liver and Biliary System* (11th ed.), Oxford, UK: Blackwell, 2002, p. 127–140.